

Article

Self-Adjoint Extension Approach to Motion of Spin-1/2 Particle in the Presence of External Magnetic Fields in the Spinning Cosmic String Spacetime

Márcio M. Cunha  and Edilberto O. Silva * 

Departamento de Física, Universidade Federal do Maranhão, 65085-580 São Luís, Maranhão, Brazil; marciomc05@gmail.com

* Correspondence: edilberto.silva@ufma.br

Received: 12 September 2020; Accepted: 2 November 2020; Published: 4 November 2020



Abstract: In this work, we study the relativistic quantum motion of an electron in the presence of external magnetic fields in the spinning cosmic string spacetime. The approach takes into account the terms that explicitly depend on the particle spin in the Dirac equation. The inclusion of the spin element in the solution of the problem reveals that the energy spectrum is modified. We determine the energies and wave functions using the self-adjoint extension method. The technique used is based on boundary conditions allowed by the system. We investigate the profiles of the energies found. We also investigate some particular cases for the energies and compare them with the results in the literature.

Dataset License: license under which the data set is made available (CC0, CC-BY, CC-BY-SA, CC-BY-NC, etc.)

Keywords: cosmic string; relativistic landau quantization; self-adjoint extension; noninertial effects

1. Introduction

The concept of singularity is an essential one in several branches of Mathematics and Physics. In Mathematics, it appears, for instance, in the study of differential equations, geometry, and topology [1]. In Physics, it can show up in the mathematical machinery describing phenomena of interest, or it can be a singularity intrinsically involved in the physical system [2]. For example, the spacetime itself can contain singularities due to the presence of black holes [3] or topological defects of cosmological origin [4].

It is common sense that the physical properties of a given system depend on the form of spacetime where it is inserted. The presence of curvature or torsion, for instance, can affect such properties. Even the light propagation can be influenced under such conditions [5], which can be understood by the notion of geodesics [6]. A particularly relevant case involving curved spacetimes and singularities occur when a topological defect shows up in producing a singularity associated with a conical space [7]. A wide range of works has dedicated attention to the issue of describing how physical quantities of interest are affected by the influence of a conical spacetime. It happens because the conical geometry can take place in many different contexts. Examples of this can be found in the study of the propagation of optical beams [8] and in research on the existence of graphite nanocones and microcones [9]. In addition, oxide graphene membranes with conical channels can be used for ultrafast water transport [10]. In condensed matter physics, a topological defect known as disclination is associated with the conical geometry. It appears, for example, in studying Liquid Crystals [11,12]. It is possible to understand the formation of a disclination from a flat material by employing the process of Volterra [13]. In this

process, a circular sector of material can be inserted into the sample or removed from it, and thus constructing a conical surface.

While a disclination is related to materials, there is an analog of such defect that occurs in spacetime: the cosmic string. The latter consists of a linear defect, whose spacetime around it is globally conical. Concerning the origin of these defects, it is believed that they were generated due to phase transitions in the early Universe [14]. They are theoretically predicted in many models in particle physics and are expected to create gravitational waves. In the case that this hypothesis is confirmed, it could provide us an extraordinary tool to study the history of the Universe [15]. A discussion about the search for signatures of cosmic strings from an observational point of view can be encountered in [16]. In cylindrical coordinates (r, φ, z) , the line element of a cosmic string is written as

$$ds^2 = dt^2 - dr^2 - \alpha^2 r^2 d\varphi^2 - dz^2. \quad (1)$$

In this expression, $r \geq 0$, $-\infty < z < \infty$, and $0 \leq \varphi \leq 2\pi$. The parameter α tells us about the presence of a conical geometry, providing an idea of how much the flat spacetime was affected by the presence of the topological defect. It is associated with the \tilde{m} , the mass per unit length of the cosmic string. More explicitly, $\alpha = 1 - 4\tilde{m}$ and it is defined in the interval $(0, 1]$. Thus, the case $\alpha = 1$ refers to the flat Minkowski spacetime in cylindrical coordinates [17]. This metric also can be imagined as a spacetime containing a conical singularity located at the origin, $r = 0$ [18]. It can be expressed in terms of the unique non-vanishing component of the curvature tensor

$$R_{r,\varphi}^{r,\varphi} = \frac{1-\alpha}{4\alpha} \delta^{(2)}(r), \quad (2)$$

where $\delta^{(2)}$ indicates the two-dimensional Dirac delta function. The line element describing a disclination is identical to that of the Equation (1), but this time we can think the parameter α as the angular deficit which comes from the Volterra process. Since we made this comparison between disclinations and cosmic strings, at this point, it is worth noting that it is possible to employ the framework of Riemann–Cartan geometry to model defects in solids, as pointed by Katanaev and Volovich [19]. A curious connection between condensed matter systems and general relativity was opened [20].

Both disclinations and cosmic strings have been considered as a background for studying several physical systems. The study of quantum systems is especially a stimulating issue because uncommon characteristics in such systems can take place when compared to the classical scenario. For example, the gravitational field near cosmic strings can produce effects on quantum fields like vacuum polarisation and particle production [21]. The influence of this background was also considered in the analysis of electron–positron pair production [22], in the Casimir effect [23], and in the relativistic hydrogen atom model [24]. The appearance of geometric phases in the conical geometry is also a subject of study in this context. Some realizations can be found in the study of graphene with disclinations [25] and in the analysis of the two-level atom model in the spacetime of a cosmic string [26]. More recently, the notion of quantum entanglement in the spacetime of a cosmic string also has been analyzed [27,28].

Besides these aspects involving quantum systems in the conical spacetime background, another important question in this context is related to the presence of electromagnetic interactions. Contributions in this direction appear in the study of Landau levels for a non-relativistic electron in the presence of disclinations [29] and in the solution of the two-dimensional electron gas problem [30]. Other interesting works were also developed in this context as, for example, the determination of the low-energy spectrum of graphene with a disclination [31], the study of the relativistic quantum motion of spin-0 and spin-1/2 particles in the spacetime of a cosmic string [32], and also problems including the Aharonov–Bohm potential [33,34].

Up to now, we have mentioned examples dealing with the quantum description of a system in the presence of disclinations and cosmic strings. In most of these works, the main objective is to show that the topological defect affects the physical properties of the system, such as the energy levels of

wave functions. These effects are observed even in the $r \neq 0$ region. However, since the $r = 0$ region presents a singularity in conical spacetime, the quantum mechanical description for this problem requires a more appropriate mathematical formulation of quantum mechanics. More explicitly, if we are interested in also describing the behavior of a quantum system at $r = 0$, we need to employ the self-adjoint approach [35–42]. It is necessary since the quantum operators which describe the physical observables are not well defined in such region: such operators are not self-adjoint, as it should be. For instance, if we are interested in obtaining the energy spectrum of a given system, we will need to proceed by making the self-adjoint extension of the Hamiltonian [43]. At this point, it is worth mentioning that, besides the self-adjoint extension method, there is another way to deal with singularities in quantum mechanics. More specifically, it is also possible to employ the framework of the Weyl–Heisenberg integral quantization [44]. While the self-adjoint extension method deals with singularities by starting with a quantum mechanical description, the Weyl–Heisenberg quantization provides a way to quantize a classical system. In that quantization procedure, the singularities might be removed. Further details and information on the Weyl–Heisenberg method can be found in the literature [45–48].

Similar to the electromagnetic interactions, the investigation of noninertial effects in the context of the conical geometry has attracted attention, and curious theoretical predictions have been achieved. These characteristics are found, for example, in the study of the relativistic quantum motion of scalar bosons [49], in the description of the two-dimensional electron gas model [50], in the relativistic Landau quantization [51], and problems involving the Dirac oscillator [52–54].

Although there is a rich literature dealing with several quantum systems in the spinning cosmic string spacetime, there is a lack of works related to the application of the self-adjoint approach considering this background. Motivated by this fact, in this paper, we study the problem of a spin-1/2 particle in such a scenario. Having in mind the importance of the electromagnetic interactions, we also include the presence of a uniform magnetic field and the Aharonov–Bohm effect. In Section 2, we present the algebraic ingredients necessary for obtaining the Dirac equation in the spinning cosmic string background. We define the field configuration involved, and using appropriate eigenfunctions and spinor decomposition, we find the radial equation of motion of the model. In Section 3, we review some basic properties and concepts of the self-adjoint extension method and write the boundary condition to be employed in solving the equation of eigenvalues. In Section 4, we apply the boundary condition to the problem and find a relation that allows us to find the energies of the particle. We study the spectrum in detail and compare it with results in the literature. We finish this section by analyzing some particular cases for the model studied. We make our concluding remarks in Section 5.

2. Dirac Equation in the Spinning Cosmic String Spacetime

In this section, we present the physical environment necessary to write the Dirac equation in curved spacetime. The first step is to obtain Dirac’s Hamiltonian in the spinning cosmic string background. We already wrote the line element for a static cosmic string spacetime. Now, we shall introduce the presence of rotation. Since we are dealing with cylindrical symmetry, the rotation is related to the coordinates t and φ . Explicitly, the metric tensor that describes this spacetime is a generalization of the metric (1), which is written as [55]

$$ds^2 = (dt + a d\varphi)^2 - dr^2 - \alpha^2 r^2 d\varphi^2 - dz^2, \quad (3)$$

where a is the parameter that describes the rotation, which depends on the angular momentum J of the cosmic string through the relation $a = 4J$. A crucial difference between (1) and (3) is that the latter allows the existence of closed timelike curves when $r < |a|/\alpha$. In this manuscript, we are not interested in considering such curves.

To study the relativistic quantum motion of an electron interacting with external magnetic fields in the metric spacetime (3), we need to write the generic Dirac equation in a curved space, given by

$$[i\gamma^\mu(x) (\nabla_\mu + ieA_\mu(x)) - M] \Psi(x) = 0, \tag{4}$$

where M represents the mass of the particle, $A_\mu(x)$ is the four-potential of the electromagnetic field, $\gamma^\mu(x)$ are the Dirac matrices in the curved space, and ∇_μ is the covariant derivative for fermion fields, which is defined by

$$\nabla_\mu = \partial_\mu + \Gamma_\mu(x), \tag{5}$$

with $\Gamma_\mu(x)$ being the spin affine connection, which can be calculated through the relation

$$\Gamma_\mu(x) = \frac{1}{4} \gamma^a \gamma^b e_a^\nu(x) [\partial_\mu e_{b\nu}(x) - \Gamma_{\mu\nu}^\sigma e_{b\sigma}(x)], \tag{6}$$

where $\Gamma_{\mu\nu}^\sigma$ are the Christoffel symbols of the second kind and $e_a^\mu(x)$ is the tetrad field to be defined later. The matrices $\gamma^\mu(x)$ are related to the usual Dirac matrices γ^a (in the flat spacetime) through the expression

$$\gamma^\mu(x) = e_a^\mu(x) \gamma^a, \tag{7}$$

with $e_a^\mu(x)$ being the tetrad field, which obeys the relations

$$e_\mu^a(x) e_\nu^b(x) \eta_{ab} = g_{\mu\nu}(x), \tag{8}$$

$$e_\mu^a(x) e_b^\mu(x) = \delta_b^a, \tag{9}$$

$$e_a^\mu(x) e_\nu^a(x) = \delta_\nu^\mu. \tag{10}$$

In the expressions above and along the manuscript, $(a, b = 0, 1, 2, 3)$ are the indices which indicate the local reference frame while $(\mu, \nu = 0, 1, 2, 3)$ indicate the curved spacetime. More precisely, we use the Greek letters to represent the tensor indices while the Latin letters are denoting Minkowski indices. The matrices $\gamma^a = (\gamma^0, \gamma^i)$ are given by

$$\gamma^0 = \begin{pmatrix} 1 & 0 \\ 0 & -1 \end{pmatrix}, \quad \gamma^i = \begin{pmatrix} 0 & \sigma^i \\ -\sigma^i & 0 \end{pmatrix}, \tag{11}$$

where $\sigma^i = (\sigma^1, \sigma^2, \sigma^3)$ indicates the standard Pauli matrices. The matrices (7) satisfy the following property:

$$\{\gamma^\mu(x), \gamma^\nu(x)\} = 2g^{\mu\nu}(x). \tag{12}$$

We use the tetrad basis and its inverse defined as [55]

$$e_\mu^a(x) = \begin{pmatrix} 1 & 0 & a & 0 \\ 0 & \cos \varphi & -r\alpha \sin \varphi & 0 \\ 0 & \sin \varphi & r\alpha \cos \varphi & 0 \\ 0 & 0 & 0 & 1 \end{pmatrix}, \quad e_a^\mu(x) = \begin{pmatrix} 1 & \frac{a \sin \varphi}{r\alpha} & -\frac{a \cos \varphi}{r\alpha} & 0 \\ 0 & \cos \varphi & \sin \varphi & 0 \\ 0 & -\frac{\sin \varphi}{r\alpha} & \frac{\cos \varphi}{r\alpha} & 0 \\ 0 & 0 & 0 & 1 \end{pmatrix}. \tag{13}$$

In the absence of rotation, we recover the tetrad basis used in Refs. [56–58]. For the tetrad field above, the affine connection is found to be

$$\Gamma_\mu = (0, 0, \Gamma_\varphi, 0), \tag{14}$$

with

$$\Gamma_\varphi = \frac{i}{2} (1 - \alpha) \Sigma^z, \tag{15}$$

where

$$\Sigma^z = \begin{pmatrix} \sigma^z & 0 \\ 0 & \sigma^z \end{pmatrix}, \quad \sigma^z = \begin{pmatrix} 1 & 0 \\ 0 & -1 \end{pmatrix}. \tag{16}$$

Note that, for the particular choice of the tetrad (13), the affine connection is identically null when $\alpha = 1$ (flat space). In the tetrad basis (13), the matrices (7) can be written explicitly as

$$\gamma^t = e_0^t \gamma^0 = \gamma^0 - a\gamma^\varphi = \gamma^0 - \frac{a}{\alpha r} \left(-\gamma^1 \sin \varphi + \gamma^2 \cos \varphi \right), \tag{17}$$

$$\gamma^r = e_a^r \gamma^a = e_0^r \gamma^0 + e_1^r \gamma^1 + e_2^r \gamma^2 = \gamma^1 \cos \varphi + \gamma^2 \sin \varphi, \tag{18}$$

$$\gamma^\varphi = e_a^\varphi \gamma^a = e_0^\varphi \gamma^0 + e_1^\varphi \gamma^1 + e_2^\varphi \gamma^2 = \frac{1}{\alpha r} \left(-\gamma^1 \sin \varphi + \gamma^2 \cos \varphi \right), \tag{19}$$

$$\gamma^z = e_0^z \gamma^0 = \gamma^3. \tag{20}$$

We can also define the α^i matrices¹, which can be written in terms of Pauli's matrices as

$$\alpha^i(x) = e_a^i(x) \begin{pmatrix} 0 & \sigma^a \\ \sigma^a & 0 \end{pmatrix} = \begin{pmatrix} 0 & \sigma^i \\ \sigma^i & 0 \end{pmatrix}, \tag{21}$$

where $\sigma^i = (\sigma^r, \sigma^\varphi, \sigma^z)$ are the Pauli matrices in cylindrical coordinates written on the tetrad basis $e_\mu^a(x)$. Such matrices are explicitly written as

$$\sigma^r = \begin{pmatrix} 0 & e^{-i\varphi} \\ e^{+i\varphi} & 0 \end{pmatrix}, \quad \sigma^\varphi = \frac{1}{r\alpha} \begin{pmatrix} 0 & -ie^{-i\varphi} \\ ie^{+i\varphi} & 0 \end{pmatrix}, \quad \sigma^z = \begin{pmatrix} 1 & 0 \\ 0 & -1 \end{pmatrix}. \tag{22}$$

We already have the geometric tools we need to describe the quantum motion of the electron in the spinning cosmic string background. Now, we need to define the magnetic interaction. Since the system exhibits symmetry of translation with respect to z direction, we can assume $p_z = z = 0$, which leads just to a plane motion [42,59–61]. We consider the particle in the presence of a potential vector superposition (in the Coulomb gauge) given by

$$\mathbf{A} = (0, A_\varphi, 0), \tag{23}$$

where A_φ is given in terms of the potential that gives rise to the uniform magnetic field plus the potential that describes the Aharonov–Bohm effect as

$$A_\varphi = -(A_1 + A_2), \tag{24}$$

$$A_1 = \frac{1}{2}\alpha Br^2, \quad A_2 = \frac{\phi}{e}, \tag{25}$$

with B being the magnitude of the uniform magnetic field, $\phi = \Phi/\Phi_0$, where Φ is the magnetic flux and $\Phi_0 = 2\pi/e$ is the quantized magnetic flux related to the Aharonov–Bohm potential. The magnetic fields associated with the Equation (25) are found to be

$$B = B_1 + B_2, \quad B_1 = B, \quad B_2 = \frac{\phi}{e} \frac{\delta(r)}{\alpha r}, \tag{26}$$

where B_1 corresponds to the uniform magnetic field and B_2 to the Aharonov–Bohm flux tube. Note that the magnetic field B_2 is given in terms of the δ function, which is a short-range potential. We are interested in analyzing the electron motion including the $r = 0$ region, in such a way that the field

¹ Do not confuse the Greek letter α used to represent the matrices of Dirac α^i and the parameter α in the metric (3).

B_2 cannot be neglected in the approach. In other words, we need to solve the Dirac equation taking into account irregular solutions at the origin. From this point, we will be interested in obtaining the radial equation for the problem. After this step, we will discuss the inclusion of the δ function in the equation of motion in more detail. Assuming the time-dependence of the eigenfunctions in the form $e^{-i\mathcal{E}t}$ and decomposing the spinor

$$\Psi(r, \varphi) = \begin{pmatrix} \psi(r, \varphi) \\ \chi(r, \varphi) \end{pmatrix}, \tag{27}$$

we find the following matrix equation:

$$\mathcal{E} \begin{pmatrix} \psi \\ \chi \end{pmatrix} - a\mathcal{E}\alpha^\varphi \begin{pmatrix} \psi \\ \chi \end{pmatrix} + \alpha^i (i\partial_i - eA_i) \begin{pmatrix} \psi \\ \chi \end{pmatrix} - \frac{1}{2} (1 - \alpha) \alpha^\varphi \Sigma^z \begin{pmatrix} \psi \\ \chi \end{pmatrix} - M\sigma^z \begin{pmatrix} \psi \\ \chi \end{pmatrix} = 0. \tag{28}$$

As the potential vector \mathbf{A} only has the component A_φ (Equation (23)), Equation (28) can be written as

$$(\mathcal{E} - M) \psi + \sigma^r i\partial_r \chi + \sigma^\varphi \left(i\partial_\varphi - eA_\varphi - a\mathcal{E} - \frac{1}{2} (1 - \alpha) \sigma^z \right) \chi = 0, \tag{29}$$

$$(\mathcal{E} + M) \chi + \sigma^i i\partial_r \psi + \sigma^\varphi \left(i\partial_\varphi - eA_\varphi - a\mathcal{E} - \frac{1}{2} (1 - \alpha) \sigma^z \right) \psi = 0, \tag{30}$$

which can still be written as

$$(\mathcal{E} - M) \psi + i\sigma^r \left(\partial_r - \frac{(1 - \alpha)}{2\alpha r} \right) \chi + i\sigma^\varphi (\partial_\varphi + ieA_\varphi + ia\mathcal{E}) \chi = 0, \tag{31}$$

$$(\mathcal{E} + M) \chi + i\sigma^r \left(\partial_r - \frac{(1 - \alpha)}{2\alpha r} \right) \psi + i\sigma^\varphi (\partial_\varphi + ieA_\varphi + ia\mathcal{E}) \psi = 0. \tag{32}$$

Equations (31) and (32) allow us to obtain a second order equation for both ψ and χ with the requirement that $\mathcal{E} \neq M$. We chose to study the equation for ψ . By isolating χ in Equation (32) and replacing in Equation (31), we obtain

$$H\psi = k^2\psi, \tag{33}$$

where

$$H = -\partial_r^2 - \frac{1}{r}\partial_r - \frac{\mathcal{L}^2}{\alpha^2 r^2} + \frac{e}{\alpha r} \sigma^z (\partial_r A_\varphi) \tag{34}$$

is the Dirac hamiltonian and

$$\mathcal{L} = \partial_\varphi + ieA_\varphi + i\frac{(1 - \alpha)}{2} \sigma^z + ia\mathcal{E}. \tag{35}$$

Making use of the underlying rotational symmetry expressed by the fact that $[H, J_z] = 0$, where

$$J_z = -i\partial_\varphi + \frac{1}{2}\sigma^z \tag{36}$$

is the total angular momentum operator in the z-direction, we decompose the Hilbert space $\mathcal{H} = L^2(\mathbb{R}^2)$ with respect to the angular momentum $\mathcal{H} = \mathcal{H}_r \otimes \mathcal{H}_\varphi$, where $\mathcal{H}_r = L^2(\mathbb{R}^+, r dr)$ and $\mathcal{H}_\varphi = L^2(\mathcal{S}^1, d\varphi)$, with \mathcal{S}^1 denoting the unit sphere in \mathbb{R}^2 . Thus, it is possible to express the eigenfunctions of the two-dimensional Hamiltonian in terms of the eigenfunctions of J_z as

$$\Psi(r, \varphi) = \begin{pmatrix} \psi(r, \varphi) \\ \chi(r, \varphi) \end{pmatrix} = \begin{pmatrix} e^{im\varphi} f_+(r) \\ ie^{i(m+1)\varphi} f_-(r) \end{pmatrix}, \tag{37}$$

where $m = 0, \pm 1, \pm 2, \pm 3, \dots$ is the angular momentum quantum number. Substituting (37) in Equation (33) together with Equations (25) and (26), we obtain the following equations:

$$H_{\pm} f_{\pm} = k_{\pm}^2 f_{\pm}, \tag{38}$$

with

$$H_+ = h_+ - \frac{\phi \delta(r)}{\alpha r}, \tag{39}$$

$$H_- = h_- + \frac{\phi \delta(r)}{\alpha r}, \tag{40}$$

and

$$h_{\pm} = -\frac{d^2}{dr^2} - \frac{1}{r} \frac{d}{dr} + \frac{J_{\pm}^2}{r^2} + \omega^2 r^2, \tag{41}$$

where

$$J_+ = \frac{1}{\alpha} \left(m - \phi + \frac{(1-\alpha)}{2} + a\mathcal{E} \right), \tag{42}$$

$$J_- = \frac{1}{\alpha} \left(m + 1 - \phi - \frac{(1-\alpha)}{2} + a\mathcal{E} \right), \tag{43}$$

represent the effective angular momenta and

$$k_+^2 = \mathcal{E}^2 - M^2 + 2\omega(J_+ + 1), \tag{44}$$

$$k_-^2 = \mathcal{E}^2 - M^2 + 2\omega(J_- - 1), \tag{45}$$

where $\omega = M\omega_c$, with $\omega_c = eB/2M$ being the cyclotron frequency. We can notice the presence of the δ function potential in Equations (39) and (40). The operator H_{\pm} is a relativistic generalization of the Landau quantization in the presence of the spin-1/2 Aharonov–Bohm effect for the case where the particle is subject to both topological and noninertial effects. As pointed out by Hagen [62], the Aharonov–Bohm effect possesses an exact equivalence with the Aharonov–Casher effect for spin-1/2 particles. Such equivalence is guaranteed just when we consider the spin of the particle in the approach. When we wish to study these models considering the spin of the particle, the following requirement arises: the term involving the δ function in the operator H_{\pm} cannot be neglected. It is known in the literature that the presence of such interaction guarantees the existence of bound states in Aharonov–Bohm-type systems [60,61,63–66]. Then, we shall solve Equation (38) for bound states using the self-adjoint extension technique [35].

3. Self-Adjoint Extension

In this section, we study the dynamics of the system in all space, including the $r = 0$ region. We consider the problem of bound states, by employing the self-adjoint extension method in the treatment. As is well known, if the Hamiltonian has a point-like singularity, as is the case of the Hamiltonian in Equation (38), we shall verify that it is self-adjoint in the region of interest. Let us consider two arbitrary operators \mathcal{A} and \mathcal{B} . If the domain of \mathcal{A} contains the domain of \mathcal{B} , or more formally, $\mathcal{D}(\mathcal{A}) \supseteq \mathcal{D}(\mathcal{B})$, and in the domain of \mathcal{B} the operators are equals, then we can state that the operator \mathcal{A} is an extension of the the operator \mathcal{B} . In this configuration, if the domain of the operator \mathcal{A} is dense, then for each vector Φ in this domain, there is a sequence Φ_n , so that we have $\Phi_n \rightarrow \Phi$.

Hence, the domain of its adjoint \mathcal{A}^\dagger , is the set of all vectors Φ for which there is a vector $\mathcal{A}^\dagger\Phi$ satisfying the relation $(\Lambda, \mathcal{A}^\dagger\Phi) = (\mathcal{A}\Lambda, \Phi)$ for all vectors $\Lambda \in \mathcal{D}(\mathcal{A})$. From this relation, we define $\mathcal{A}^\dagger\Phi$. We can also establish that an operator \mathcal{A} with dense domain is symmetric if $(\Lambda, \mathcal{A}\Phi) = (\mathcal{A}\Lambda, \Phi)$ for every Λ and Φ in its domain. In this case, $\mathcal{A}^\dagger\psi$ can be defined as $\mathcal{A}^\dagger\Phi = \mathcal{A}\Phi$ for all $\Phi \in \mathcal{D}(\mathcal{A})$, and \mathcal{A}^\dagger is said to be an extension of \mathcal{A} . If $\mathcal{A}^\dagger = \mathcal{A}$, then \mathcal{A} is called self-adjoint operator or Hermitian operator. It is important to note that a symmetric operator can fail to be a self-adjoint operator. For the operator \mathcal{A} to be a self-adjoint operator, it has to be symmetric, $\mathcal{A} = \mathcal{A}^\dagger$, and the domains of the operator and its adjoint have to be equal as well, i.e., $\mathcal{D}(\mathcal{A}) = \mathcal{D}(\mathcal{A}^\dagger)$.

According to the above definitions, the operator h_\pm , with domain $\mathcal{D}(h_\pm)$ is said to be self-adjoint if and only if $h_\pm = h_\pm^\dagger$, $\mathcal{D}(h_\pm) = \mathcal{D}(h_\pm^\dagger)$, with h_\pm^\dagger being the adjoint of operator h_\pm and, moreover, it has to be symmetrical. In addition, for smooth functions, $\mathcal{F} \in C_0^\infty(\mathbb{R}^2)$, with $\mathcal{F}(0) = 0$, we should have $H_\pm\mathcal{F} = h_\pm\mathcal{F}$. In this case, it is possible to interpret H_\pm as a self-adjoint extension of $h_\pm|_{C_0^\infty(\mathbb{R}^2/\{0\})}$ [64,67,68]. The self-adjoint extension method consists in extending the domain of $\mathcal{D}(h_\pm)$ in order to match $\mathcal{D}(h_\pm^\dagger)$. It is known that the operator h_\pm is essentially self-adjoint for $|J_\pm| \geq 1$, while, for $|J_\pm| < 1$, it admits a one-parameter family of self-adjoint extensions [35], said h_{\pm,ζ_m} , where ζ_m is the self-adjoint extension parameter of the problem. To characterize this family, we shall use the approach developed in Refs. [69,70], which is based on the boundary conditions at the origin. All the self-adjoint extensions h_{\pm,ζ_m} of h_\pm are parametrized by the boundary condition at the origin

$$\Omega_0 = \zeta_m\Omega_1, \tag{46}$$

with

$$\Omega_0 = \lim_{r \rightarrow 0^+} r^{|J_\pm|} f_\pm(r), \tag{47}$$

$$\Omega_1 = \lim_{r \rightarrow 0^+} \frac{1}{r^{|J_\pm|}} \left[f_\pm(r) - \Omega_0 \frac{1}{r^{|J_\pm|}} \right], \tag{48}$$

where $\zeta_m \in \mathbb{R}$ is the self-adjoint extension parameter. Physically, it is known that the quantity $1/\zeta_m$ can be interpreted as the scattering length of h_{\pm,ζ_m} (More details on this issue are given in Ref. [70]). For $\zeta_m = \infty$, the boundary condition represents the Friedrichs extension of h_\pm . In the case of Equation (38), it means that we are studying the Dirac equation without taking into account terms that explicitly depend on the spin of the particle, with regular wave functions at the origin ($\Psi(0) = 0$). This situation is analogous to imposing the Dirichlet boundary condition on the wave function $\Psi(r, \varphi)$, which allows us to recover the original results of Ref. [71]. On the other hand, if we consider $|\zeta_m| < \infty$, the operator h_\pm characterizes a point interaction at $r = 0$ region. In this case, the boundary condition permits a $r^{-|J_\pm|}$ singularity in the wave functions at this point [72] (we show this in the next section). For $\zeta_m = 0$, we have the free Hamiltonian H_\pm (without the δ function). For this last case, the boundary condition reveals that only regular wave functions at the origin are considered. According to the theory of self-adjoint extensions, we can not impose any boundary condition without discovering which boundary conditions are allowed to Equation (38) [35]. For the model in question, the operator h_\pm is one that satisfies the boundary condition (46). Another question that needs to be clarified here is related to the choice of the parameter ζ_m . Since we are dealing with a non-confined relativistic quantum system, we must ensure that $\Psi(r, \varphi)$ is finite in the range $(0, \infty)$, which is a necessary and sufficient condition for it to be square-integrable and also to ensure the existence of bound state solutions.

4. The Energy Spectrum

In this section, we solve Equation (38) in the $r \neq 0$ region to determine the energies of the particle in the spinning cosmic string spacetime. By using the variable change $y = \omega r^2$, Equation (46) can be written as

$$y \frac{d^2 f_{\pm}(y)}{dy^2} + \frac{df_{\pm}(y)}{dy} - \left(\frac{J_{\pm}^2}{4y} + \frac{y}{4} - \frac{k_{\pm}^2}{4\omega} \right) f_{\pm}(y) = 0. \tag{49}$$

Due to the boundary condition in Equation (46), we shall take into account regular and irregular solutions for Equation (49). Studying the asymptotic limits of Equation (49), we obtain the following regular (+) (irregular (-)) solution:

$$f_{\pm}(y) = y^{\pm \frac{|J_{\pm}|}{2}} e^{-\frac{y}{2}} F_{\pm}(y). \tag{50}$$

Substituting this solution (Equation (50)) in Equation (49), we find

$$y \frac{d^2 F_{\pm}(y)}{dy^2} + (1 \pm |J_{\pm}| - y) \frac{dF_{\pm}(y)}{dy} - \left(\frac{1 \pm |J_{\pm}|}{2} - \frac{k_{\pm}^2}{4\omega} \right) F_{\pm}(y) = 0. \tag{51}$$

Equation (51) is a confluent hypergeometric equation type

$$z \frac{d^2 F(z)}{dz^2} + (b - z) \frac{dF(z)}{dz} - aF(z) = 0. \tag{52}$$

The general solution of Equation (51) is

$$F_{\pm}(y) = a_m \mathcal{M} \left(\frac{1}{2} (1 + |J_{\pm}|) - \frac{k_{\pm}^2}{4\omega}, 1 + |J_{\pm}|, y \right) + b_m U \left(\frac{1}{2} (1 + |J_{\pm}|) - \frac{k_{\pm}^2}{4\omega}, 1 + |J_{\pm}|, y \right), \tag{53}$$

where $\mathcal{M}(a, b, z)$ denotes the Kummer function (or confluent hypergeometric function of the first kind ${}_1F_1(a, b, z)$), while $U(a, b, z)$ represents the confluent hypergeometric function of the second kind [73], and a_m and b_m are constants of normalization. Using the property

$$U(a, b, z) = \frac{\Gamma(1 - b)}{\Gamma(a + 1 - b)} \mathcal{M}(a, b, z) + \frac{\Gamma(b - 1)}{\Gamma(a)} z^{1-b} \mathcal{M}(a + 1 - b, 2 - b, z), \tag{54}$$

the solution (53) can be fully expressed in terms of the Kummer function. Consequently, the solution (50) assumes the form

$$f_{\pm}(y) = A_m y^{\frac{|J_{\pm}|}{2}} e^{-\frac{y}{2}} \mathcal{M}(a_+, 1 + |J_{\pm}|, y) + B_m y^{-\frac{|J_{\pm}|}{2}} e^{-\frac{y}{2}} \mathcal{M}(a_-, 1 - |J_{\pm}|, y), \tag{55}$$

where A_m and B_m are, respectively, the coefficients of the regular and irregular solutions at the origin, and

$$a_+ = \frac{1}{2} (1 + |J_{\pm}|) - \frac{k_{\pm}^2}{4\omega}, \tag{56}$$

$$a_- = \frac{1}{2} (1 - |J_{\pm}|) - \frac{k_{\pm}^2}{4\omega}. \tag{57}$$

Now, we will apply the contour condition (46) to the problem. We need to use the solution (55) together with the series expansion until first order in y for the function $\mathcal{M}(a_{\pm}, 1 \pm |J_{\pm}|, y)$, given by

$$\mathcal{M}(a_+, 1 + |J_{\pm}|, \omega r^2) = 1 + \frac{a_+ \omega}{1 + |J_{\pm}|} r^2 + \dots, \tag{58}$$

$$\mathcal{M}(a_-, 1 - |J_{\pm}|, \omega r^2) = 1 + \frac{a_- \omega}{1 - |J_{\pm}|} r^2 + \dots \tag{59}$$

After some intermediate steps, we obtain the following relation between the coefficients A_m and B_m :

$$\zeta_m \omega^{|J_{\pm}|} = \frac{B_m}{A_m} \left[1 - \left(\frac{\omega}{2} - \frac{k_{\pm}^2}{4(1 - |J_{\pm}|)} \right) \zeta_m \lim_{r \rightarrow 0^+} r^{2-2|J_{\pm}|} \right]. \tag{60}$$

By studying the $\lim_{r \rightarrow 0^+} r^{2-2|J_{\pm}|}$, we verify that it diverges if $|J_{\pm}| \geq 1$. From this condition, we can establish that B_m must be zero if $|J_{\pm}| \geq 1$ and only the regular solution contributes to $f_{\pm}(r)$. As mentioned above, if $|J_{\pm}| < 1$, we have only the situation when the operator h_{\pm} is not self-adjoint. In this case, a contribution of the irregular solution to $f_{\pm}(r)$ at the origin [61,74–79] turns up. In other words, the contribution of the irregular solution for the system wave function stems from the fact that the operator h_{\pm} is not self-adjoint.

For $f_{\pm}(r)$ be a bound state wave function, it must vanish at large values of r . In addition, it must be a normalizable wave function. These conditions allow us to obtain another relationship involving the constants A_m and B_m . Then, using the asymptotic representation of the confluent hypergeometric function for large argument,

$$\mathcal{M}(a, b, z) = \frac{\Gamma(b)}{\Gamma(a)} e^z z^{a-b} + \frac{\Gamma(b)}{\Gamma(b-a)} (-z)^{-a}, \tag{61}$$

we obtain the relation

$$\frac{B_m}{A_m} = -\frac{\omega^{\frac{|J_{\pm}|}{2}} X}{\omega^{-\frac{|J_{\pm}|}{2}} Y'}, \tag{62}$$

where

$$X = \frac{\Gamma(1 + |J_{\pm}|)}{\Gamma(a_+)} e^{\omega r^2} \omega^{a_+ - 1 - |J_{\pm}|} r^{-2 + 2a_+ - |J_{\pm}|} + \frac{\Gamma(1 + |J_{\pm}|)}{\Gamma(1 + |J_{\pm}| - a_+)} (-\omega)^{-a_+} r^{|J_{\pm}|} (-r)^{-2a_+}, \tag{63}$$

$$Y = \frac{\Gamma(1 - |J_{\pm}|)}{\Gamma(a_-)} e^{\omega r^2} \omega^{a_- - 1 + |J_{\pm}|} r^{-2 + 2a_- + |J_{\pm}|} + \frac{\Gamma(1 - |J_{\pm}|)}{\Gamma(1 - |J_{\pm}| - a_-)} (-\omega)^{-a_-} r^{-|J_{\pm}|} (-r)^{-2a_-}. \tag{64}$$

Equation (62) can be simplified by studying the behavior from X and Y for $r \rightarrow \infty$. The resulting equation is

$$\frac{B_m}{A_m} = -\frac{\Gamma(1 + |J_{\pm}|)}{\Gamma(1 - |J_{\pm}|)} \frac{\Gamma\left(\frac{1}{2}(1 - |J_{\pm}|) - \frac{k_{\pm}^2}{4\omega}\right)}{\Gamma\left(\frac{1}{2}(1 + |J_{\pm}|) - \frac{k_{\pm}^2}{4\omega}\right)}. \tag{65}$$

Now, let's return to Equation (60) and consider the condition $|J_{\pm}| < 1$. It provides

$$\frac{B_m}{A_m} = \zeta_m \omega^{|J_{\pm}|}. \tag{66}$$

From Equations (65) and (66), we obtain the relation

$$\frac{\Gamma\left(\frac{1}{2}(1 + |J_{\pm}|) - \frac{k_{\pm}^2}{4\omega}\right)}{\Gamma\left(\frac{1}{2}(1 - |J_{\pm}|) - \frac{k_{\pm}^2}{4\omega}\right)} = -\frac{1}{\zeta_m \omega^{|J_{\pm}|}} \frac{\Gamma(1 + |J_{\pm}|)}{\Gamma(1 - |J_{\pm}|)}. \tag{67}$$

We can see that Equation (67) determines, implicitly, the energies of the particle for different values of ζ_m . For the present system, we investigate two values, which are related to the boundary conditions at the origin and at infinity, respectively. For $\zeta_m = 0$, when the δ function is absent, only the

regular solution contributes to the bound state wave function. For $\xi_m = \infty$, only the irregular solution contributes to the bound state wave function. For all other values of ξ_m , both regular and irregular solutions contribute to the bound state wave function. The energies for the two cases above are accessed by studying the poles of the Γ function through the relations [58,80]

$$\frac{1}{2}(1 + |J_{\pm}|) - \frac{k_{\pm}^2}{4\omega} = -n, \quad \text{for } \xi_m = 0 \quad (\text{regular solution}), \tag{68}$$

$$\frac{1}{2}(1 - |J_{\pm}|) - \frac{k_{\pm}^2}{4\omega} = -n, \quad \text{for } \xi_m = \infty \quad (\text{irregular solution}), \tag{69}$$

with $n = 0, 1, 2, \dots$. Note that, in Equations (68) and (69), the quantity J_{\pm} (see Equations (42) and (43)) is given in terms of the energy \mathcal{E} . Thus, to find an expression for the energy eigenvalues, we must consider $J_{\pm} > 0$ and $J_{\pm} < 0$, respectively, and then solve these expressions for \mathcal{E} . We obtain the following energies:

(i) For the case $\xi_m = 0$:

$$\mathcal{E}_{R,+}^{(>)} = \pm \sqrt{M^2 + 4nM\omega_c}, \quad \text{for } J_+ > 0, \tag{70}$$

$$\mathcal{E}_{R,+}^{(<)} = -\frac{2aM\omega_c}{\alpha} \pm \frac{1}{\alpha} \sqrt{(2aM\omega_c)^2 + 4\alpha^2 M\omega_c (n - j_+) + \alpha^2 M^2}, \quad \text{for } J_+ < 0, \tag{71}$$

$$\mathcal{E}_{R,-}^{(>)} = \pm \sqrt{M^2 + 4M\omega_c (n + 1)}, \quad \text{for } J_- > 0, \tag{72}$$

$$\mathcal{E}_{R,-}^{(<)} = -\frac{2aM\omega_c}{\alpha} \pm \frac{1}{\alpha} \sqrt{(2aM\omega_c)^2 + 4\alpha^2 M\omega_c (n - j_- + 1) + \alpha^2 M^2}, \quad \text{for } J_- < 0. \tag{73}$$

(ii) For the case $\xi_m = \infty$:

$$\mathcal{E}_{I,+}^{(>)} = -\frac{2aM\omega_c}{\alpha} \pm \frac{1}{\alpha} \sqrt{(2aM\omega_c)^2 + 4\alpha^2 M\omega_c (n - j_+) + \alpha^2 M^2}, \quad \text{for } J_+ > 0, \tag{74}$$

$$\mathcal{E}_{I,+}^{(<)} = \pm \sqrt{M^2 + 4nM\omega_c}, \quad \text{for } J_+ < 0, \tag{75}$$

$$\mathcal{E}_{I,-}^{(>)} = -\frac{2aM\omega_c}{\alpha} \pm \frac{1}{\alpha} \sqrt{(2aM\omega_c)^2 + 4\alpha^2 M\omega_c (n - j_- + 1) + \alpha^2 M^2}, \quad \text{for } J_- > 0, \tag{76}$$

$$\mathcal{E}_{I,-}^{(<)} = \pm \sqrt{M^2 + 4M\omega_c (n + 1)}, \quad \text{for } J_- < 0, \tag{77}$$

with

$$j_+ = \frac{1}{\alpha} \left(m - \phi + \frac{(1 - \alpha)}{2} \right), \tag{78}$$

$$j_- = \frac{1}{\alpha} \left(m + 1 - \phi - \frac{(1 - \alpha)}{2} \right). \tag{79}$$

The above energies present some curious characteristics. When we compare the energies $\mathcal{E}_{R,+}^{(>)}$ and $\mathcal{E}_{I,+}^{(<)}$, we see that they are the same. The same occurs when we compare $(\mathcal{E}_{R,+}^{(<)}, \mathcal{E}_{I,+}^{(>)})$, $(\mathcal{E}_{R,-}^{(<)}, \mathcal{E}_{I,-}^{(>)})$ and $(\mathcal{E}_{R,-}^{(>)}, \mathcal{E}_{I,-}^{(<)})$. We also notice that $\mathcal{E}_{R,\pm}^{(>)}$ and $\mathcal{E}_{I,\pm}^{(<)}$ are independent of the parameters m , α , ϕ and a while $\mathcal{E}_{R,\pm}^{(<)}$ and $\mathcal{E}_{I,\pm}^{(>)}$ are given in terms of all the physical parameters involved in the model. The energies of the regular solution (70) and (71) can be compared with the energies (47) and (50) of Ref. [55], respectively, for the particular case when the cyclotron frequency plays the role of the Dirac oscillator frequency. We make some energy sketches as a function of some parameters of the system. In all the figures, we consider $M = 1$. Because of the dependence on all the parameters of the model and the similarity with the other energies, we prefer to analyze only the energy (71). We use

solid and dashed-dotted lines to represent the energy of the particle and dashed and dotted lines to the antiparticle. In Figure 1, we investigate the profile of $\mathcal{E}_{R,+}^{(<)}$ as a function of ω_c . When $a = 0.2$, $\alpha = 0.8$ and $\phi = 0.5$, the spectrum is located in the energy range $(-1, 1)$. In addition, we also note that the energies increase when ω_c is increased or equivalently, when the magnetic field B is increased (Figure 1a). This is verified for $n = 0$ (blue color), $n = 1$ (red color) and $n = 2$ (green color) for $m = 1$ and $m = 2$ (both identified in the figures). On the other hand, when we change the curvature and the flux to $\alpha = 0.6$ and $a = 1$ and keeping the same parameter a , the spectrum assumes the profile of Figure 1b (for $m = -1$ and $m = -4$). In this case, we can see that the energies increase when n increases and m decreases. In both cases, we can also clearly see that the spectrum is not symmetrical about $\mathcal{E}_{R,+}^{(<)} = 0$. In fact, when $a = 0$ in Equations (71), (73), (74) and (76), the symmetry is recovered.

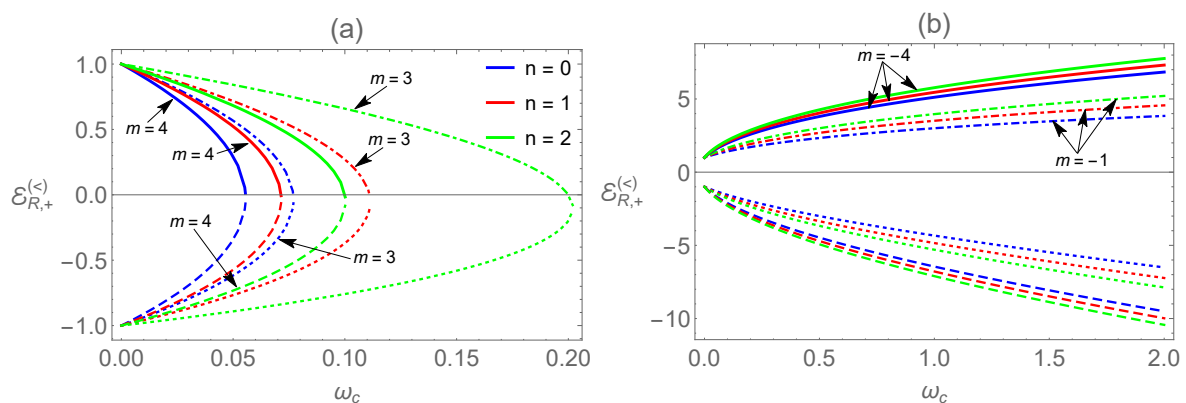


Figure 1. Sketch of the energy levels $\mathcal{E}_{R,+}^{(<)}$ (Equation (71)) as a function of ω_c . In (a), $a = 0.2$, $\alpha = 0.8$, $\phi = 0.5$. In (b), $a = 0.2$, $\alpha = 0.6$, $\phi = 1$.

When we investigate the profile of $\mathcal{E}_{R,+}^{(<)}$ as a function of α , we verify that the spectrum is negative (Figure 2). In particular, when $a = 0.8$, $\omega_c = 2$ and $\phi = 0.5$ for $m = 5$ and $m = 6$, we can see that the energies increase when α is increased and m is decreased (Figure 2a). Furthermore, energies are only allowed for $\alpha < 0.3$. In Figure 2b, we show the profile for $\omega_c = 0.4$, $\phi = 0.5$ and $m = 1$ for $\alpha = 0.4$ and $a = 0.9$. For this configuration, we see that $|\mathcal{E}_{R,+}^{(<)}|$ increases when n increases. However, when the rotation is lower, ranges of α emerge in which the energy is forbidden.

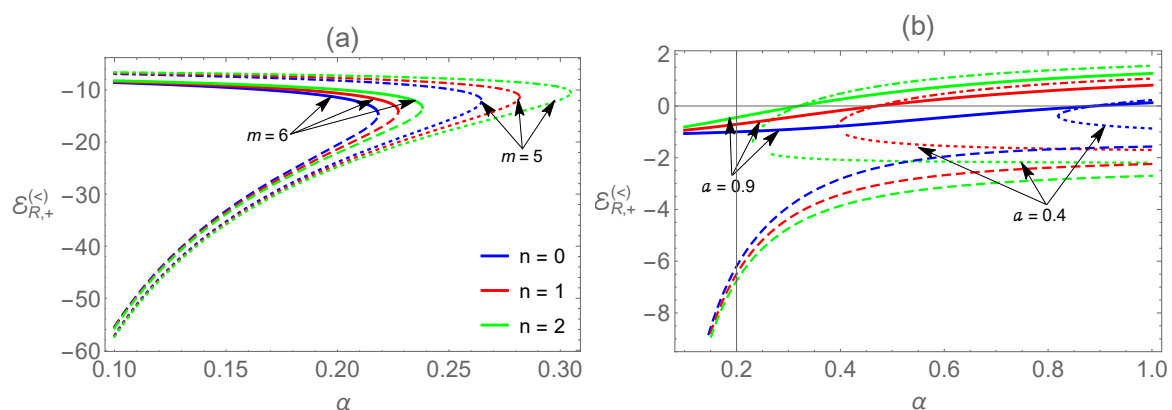


Figure 2. Sketch of the energy levels $\mathcal{E}_{R,+}^{(<)}$ (Equation (71)) as a function of α . In (a), $a = 0.8$, $\omega = 2$ and $\phi = 0.5$. In (b), $a = 0.4$, $\omega = 0.4$ and $\phi = 0.5$.

The sketch of $\mathcal{E}_{R,+}^{(<)}$ as a function of rotation is depicted in Figure 3. Considering $\alpha = 0.5$, $\omega_c = 1$ and $\phi = 2.5$, we see that the $|\mathcal{E}_{R,+}^{(<)}|$ increases when n is increased and m is decreased. For simplicity's sake, we consider $m = 0$ and $m = 2$ (Figure 3a). On the other hand, when we consider the parameters

$\omega_c = 1, \phi = 2.5$ and $m = 1$ for $\alpha = 0.4$ and $a = 0.9$, we see that the energy states of the particle (solid and dashed-dotted lines) are closer to each other while those of the antiparticle (dashed and dotted lines) are more separated when α approaches 1 (Figure 3b).

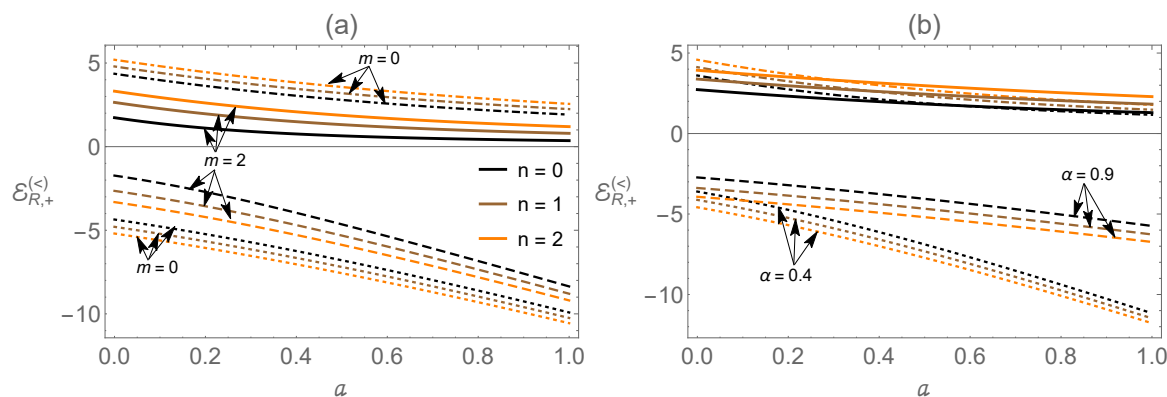


Figure 3. Sketch of the energy levels $\mathcal{E}_{R,+}^{(<)}$ (Equation (71)) as a function of a . In (a), we use $\alpha = 0.5, \phi = 2.5$ and $\omega = 1$ for $m = 0$ and $m = 2$. In (b), we use $\omega = 1, \phi = 2.5$ and $m = 1$ for $\alpha = 0.4$ and $\alpha = 0.9$.

The profile of $\mathcal{E}_{R,+}^{(<)}$ as a function of ϕ is displayed in Figure 4 considering two settings. In the first one, we use $\alpha = 0.5, \omega_c = 1$ and $a = 0.5$ for $m = 0$ and $m = 2$ (Figure 4a). As in the other cases analyzed above, we also observe an increment in the spectrum $\mathcal{E}_{R,+}^{(<)}$ when n increases. We also verify that the energy states with $m = 0$ are closer to each other while the states with $m = 2$ are more separate. In addition, a flux range appears where energy is forbidden. In the second situation, we use $\alpha = 0.2, \omega_c = 9, a = 0.1$ and keeping the same values of m . In this case, we observe that $|\mathcal{E}_{R,+}^{(<)}|$ increases as well as the flux range where the energy is forbidden.

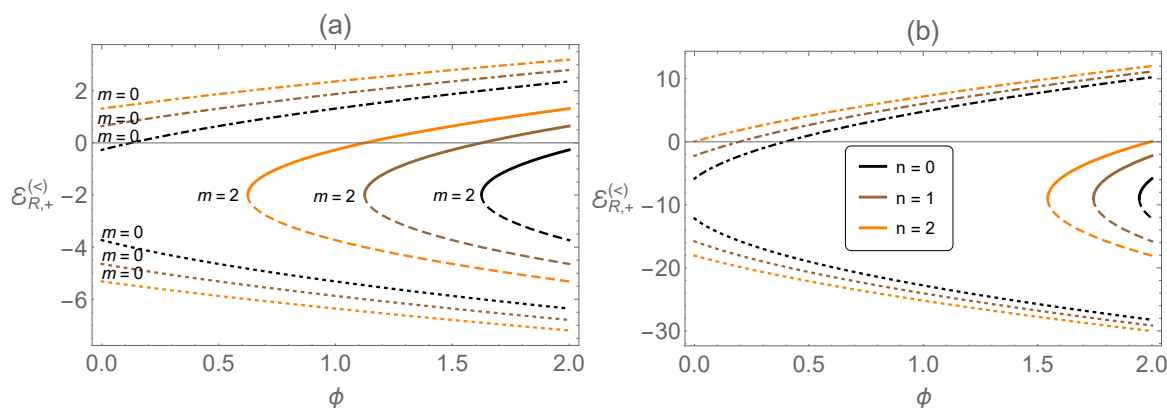


Figure 4. Sketch of the energy levels $\mathcal{E}_{R,+}^{(<)}$ (Equation (71)) as a function of ϕ . In (a), $a = 0.5, \alpha = 0.5$ and $\omega = 1$ and, In (b), $a = 0.1, \alpha = 0.2$ and $\omega = 9$.

In particular, when the rotation is null, J_{\pm} no longer depends on \mathcal{E} and Equations (68) and (69) become

$$\frac{1}{2} (1 + |j_{\pm}|) - \frac{k_{\pm}^2}{4\omega} = -n \quad \text{for } \zeta_m = 0 \quad (\text{regular solution}), \tag{80}$$

$$\frac{1}{2} (1 - |j_{\pm}|) - \frac{k_{\pm}^2}{4\omega} = -n \quad \text{for } \zeta_m = \infty \quad (\text{irregular solution}). \tag{81}$$

Solving (80) and (81) to \mathcal{E} , we obtain

$$\mathcal{E}_{R,+} = \pm \sqrt{2M\omega_c (2n + |j_+| - j_+) + M^2} \text{ (regular case),} \tag{82}$$

$$\mathcal{E}_{I,+} = \pm \sqrt{2M\omega_c (2n - |j_+| - j_+) + M^2} \text{ (irregular case),} \tag{83}$$

$$\mathcal{E}_{R,-} = \pm \sqrt{M^2 + 2M\omega_c (2n + |j_-| - j_- + 2)} \text{ (regular case),} \tag{84}$$

$$\mathcal{E}_{I,-} = \pm \sqrt{M^2 + 2M\omega_c (2n - |j_-| - j_- + 2)} \text{ (irregular case).} \tag{85}$$

According to the discussion presented in Section 3, we can state that, for $|j_{\pm}| \geq 1$ or when the δ function is absent, only the regular solution contributes to the bound state wave function. In this case, the energy is given by Equation (82). Differently, when the solution is singular at the origin, the corresponding energy is given by Equation (83). Energies (82) and (83) are equivalent to the energies (46) of Ref. [58]. Moreover, we also see that they are symmetrical around $\mathcal{E}_{\pm} = 0$ in both regular and irregular cases. As a final investigation, making $\alpha = 1$ (flat space) and $\phi = 0$ (no magnetic flux), we no longer have any curvature effect and the term involving the δ interaction is absent. In this case, only regular solutions are considered and the Equation (82) implies the usual Landau relativistic quantization [81]

$$\mathcal{E}_{R,+} = \pm \sqrt{M^2 + 2M\omega_c (2n + |m| - m)}, \tag{86}$$

$$\mathcal{E}_{R,-} = \pm \sqrt{M^2 + 2M\omega_c (2n + |m + 1| - (m + 1) + 2)}, \tag{87}$$

which is an important result that has several important applications in many branches of physics.

5. Conclusions

In the present manuscript, we have addressed the problem of the relativistic quantum motion of an electron in the spinning cosmic string background in the presence of a uniform magnetic field and the Aharonov–Bohm potential. The new ingredients in the study of this model are the inclusion of the spin degree of freedom and the solution of the quantum motion equation by using the self-adjoint extension method. We have written the Dirac equation describing the model (Equation (28)) and derived the second-order equation for the upper component of the spinor (Equation (33)).

We have used an appropriate ansatz (Equation (37)) and obtained the radial equation corresponding to the bispinor (Equation (38)). The radial equation includes the δ function which arises due to the interaction between the magnetic field and the particle spin at $r = 0$. The inclusion of spin effects in the solution of the problem is also the reason why the particle can access the $r = 0$ region in the model studied. We have shown that this process requires that irregular solutions at the $r = 0$ shall be considered in the treatment of the problem. Having this in mind, we have employed the self-adjoint extension method based on boundary conditions at the origin (Equation (46)). The boundary condition revealed to us that the operator h_{\pm} is self-adjoint only if $|J_{\pm}| \geq 1$. Outside this range, i.e., for $|J_{\pm}| < 1$, h_{\pm} is not self-adjoint. The boundary condition (46) and the analysis of the asymptotic behavior of the solution $f_{\pm}(y)$ (Equation (55)) both allowed us to obtain a relation between the constants A_m and B_m . As a result, we obtained a relation that allowed us to find the energies of the particle in terms of the self-adjoint extension parameter, ζ_m . We have considered two values for ζ_m , which are related to the boundary conditions at the $r = 0$ and at the infinity, namely $\zeta_m = 0$ and $\zeta_m = \infty$. For each of these conditions, we find the corresponding energy for the particle.

The presence of non-inertial effects shows us that the energy spectrum of the particle is given by eight equations (Equations (70)–(77)). However, we have identified by direct comparison that the energies $(\mathcal{E}_{R,+}^{(>)}, \mathcal{E}_{I,+}^{(<)})$, $(\mathcal{E}_{R,+}^{(<)}, \mathcal{E}_{I,+}^{(>)})$, $(\mathcal{E}_{R,-}^{(<)}, \mathcal{E}_{I,-}^{(>)})$ and $(\mathcal{E}_{R,-}^{(>)}, \mathcal{E}_{I,-}^{(<)})$ are equals. We have found that the energies $\mathcal{E}_{R,\pm}^{(>)}$ and $\mathcal{E}_{I,\pm}^{(<)}$ depend only on M , n and ω_c while the energies $\mathcal{E}_{R,\pm}^{(<)}$ and $\mathcal{E}_{I,\pm}^{(>)}$ depend on

all physical parameters of the model. We have argued that the energies $\mathcal{E}_{R,\pm}^{(>)}$ and $\mathcal{E}_{I,\pm}^{(<)}$ are symmetric about zero energy while $\mathcal{E}_{R,\pm}^{(<)}$ and $\mathcal{E}_{I,\pm}^{(>)}$ present this characteristic only in the absence of rotation. Because of the condition $|J_{\pm}| < 1$, few energy states of the particle are inside of this interval. For the model studied, only the states with $m = 0$ and $n = 0$ belong to this range. For this reason, we analyze graphically only the energy $\mathcal{E}_{R,\pm}^{(<)}$. We exhibited the profile of $\mathcal{E}_{R,\pm}^{(<)}$ as a function of ω_c , α , a and ϕ . In all cases investigated, we verified that both the curvature and rotation modify the energy levels of the particle. To finish the work, we studied some particular cases to show that the model studied is consistent with other results in the literature.

Author Contributions: E.O.S.: Conceptualization, methodology, software, supervision, writing—original draft preparation, writing—review and editing, project administration; M.M.C.: Writing—original draft preparation, formal analysis, investigation. All authors have read and agreed to the published version of the manuscript.

Funding: This work was partially supported by the Brazilian agencies CAPES, CNPq and FAPEMA. E.O.S. acknowledges CNPq Grants 427214/2016-5 and 307203/2019-0, and FAPEMA Grants 01852/14 and 01202/16. This study was financed in part by the Coordenação de Aperfeiçoamento de Pessoal de Nível Superior-Brasil (CAPES)—Finance Code 001. M.M.C. acknowledges CAPES Grant 88887.358036/2019-00.

Acknowledgments: We would like to thank R.C. (Universidade Federal do Maranhão, MA, Brazil) for his remarks and comments.

Conflicts of Interest: The authors declare no conflict of interest.

References

1. Brasselet, J.P. *Singularities in Geometry and Topology: Proceedings of the Trieste Singularity Summer School and Workshop, ICTP, Trieste, Italy, 15 August–3 September 2005*; World Scientific: Singapore, 2007.
2. Konkowski, D.A.; Helliwell, T.M. Understanding singularities—Classical and quantum. *Int. J. Mod. Phys. A* **2016**, *31*, 1641007. [[CrossRef](#)]
3. D’Inverno, R. *Introducing Einstein’s Relativity*; Clarendon Press: Oxford, UK, 1992.
4. Bäuerle, C.; Bunkov, Y.M.; Fisher, S.; Godfrin, H.; Pickett, G. Laboratory simulation of cosmic string formation in the early Universe using superfluid ^3He . *Nature* **1996**, *382*, 332–334. [[CrossRef](#)]
5. Schultheiss, V.H.; Batz, S.; Szameit, A.; Dreisow, F.; Nolte, S.; Tünnermann, A.; Longhi, S.; Peschel, U. Optics in Curved Space. *Phys. Rev. Lett.* **2010**, *105*, 143901. [[CrossRef](#)] [[PubMed](#)]
6. Radożycki, T. Geometrical optics and geodesics in thin layers. *Phys. Rev. A* **2018**, *98*, 063802. [[CrossRef](#)]
7. Vilenkin, A.; Shellard, E.P. *Cosmic Strings and Other Topological Defects*; Cambridge University Press: Cambridge, UK, 2000.
8. Zhang, Y.L.; Dong, X.Z.; Zheng, M.L.; Zhao, Z.S.; Duan, X.M. Steering electromagnetic beams with conical curvature singularities. *Opt. Lett.* **2015**, *40*, 4783–4786. [[CrossRef](#)]
9. Gogotsi, Y.; Dimovski, S.; Libera, J. Conical crystals of graphite. *Carbon* **2002**, *40*, 2263–2267. [[CrossRef](#)]
10. Ma, Y.; Su, Y.; He, M.; Shi, B.; Zhang, R.; Shen, J.; Jiang, Z. Graphene oxide membranes with conical nanochannels for ultrafast water transport. *ACS Appl. Mater. Interfaces* **2018**, *10*, 37489–37497. [[CrossRef](#)] [[PubMed](#)]
11. Denniston, C. Disclination dynamics in nematic liquid crystals. *Phys. Rev. B* **1996**, *54*, 6272–6275. [[CrossRef](#)]
12. Kleman, M. Defects in liquid crystals. *Rep. Prog. Phys.* **1989**, *52*, 555–654. [[CrossRef](#)]
13. Puntigam, R.A.; Soleng, H.H. Volterra distortions, spinning strings, and cosmic defects. *Class. Quantum Gravity* **1997**, *14*, 1129. [[CrossRef](#)]
14. Hindmarsh, M.B.; Kibble, T.W.B. Cosmic strings. *Rep. Prog. Phys.* **1995**, *58*, 477–562. [[CrossRef](#)]
15. Cui, Y.; Lewicki, M.; Morrissey, D.E.; Wells, J.D. Cosmic archaeology with gravitational waves from cosmic strings. *Phys. Rev. D* **2018**, *97*, 123505. [[CrossRef](#)]
16. Brandenberger, R.H. Searching for Cosmic Strings in New Observational Windows. *Nucl. Phys. B Proc. Suppl.* **2014**, *246–247*, 45–57. [[CrossRef](#)]
17. Svaiter, B.F.; Svaiter, N.F. Quantum processes: Stimulated and spontaneous emission near cosmic strings. *Class. Quantum Gravity* **1994**, *11*, 347–358. [[CrossRef](#)]
18. Sokoloff, D.D.; Starobinskii, A.A. On the structure of curvature tensor on conical singularities. *Dokl. Akad. Nauk* **1977**, *234*, 1043–1046.

19. Katanaev, M.O.; Volovich, I.V. Theory of defects in solids and three-dimensional gravity. *Ann. Phys.* **1992**, *216*, 1–28. [[CrossRef](#)]
20. Moraes, F. Condensed Matter Physics as a laboratory for gravitation and Cosmology. *Braz. J. Phys.* **2000**, *30*, 304–308. [[CrossRef](#)]
21. Davies, P.C.W.; Sahni, V. Quantum gravitational effects near cosmic strings. *Class. Quantum Gravity* **1988**, *5*, 1. [[CrossRef](#)]
22. Skarzhinsky, V.D.; Harari, D.D.; Jasper, U. Quantum electrodynamics in the gravitational field of a cosmic string. *Phys. Rev. D* **1994**, *49*, 755–762. [[CrossRef](#)]
23. Moraes, F. Casimir effect around disclinations. *Phys. Lett. A* **1995**, *204*, 399–404. [[CrossRef](#)]
24. Marques, G.D.; Bezerra, V.B. Hydrogen atom in the gravitational fields of topological defects. *Phys. Rev. D* **2002**, *66*, 105011. [[CrossRef](#)]
25. Furtado, C.; Moraes, F.; de M. Carvalho, A. Geometric phases in graphitic cones. *Phys. Lett. A* **2008**, *372*, 5368–5371. [[CrossRef](#)]
26. Cai, H.; Ren, Z. Geometric phase for a static two-level atom in cosmic string spacetime. *Class. Quantum Gravity* **2018**, *35*, 105014. [[CrossRef](#)]
27. Huang, Z.; He, Z. Quantum entanglement in the background of cosmic string spacetime. *Quantum Inf. Process.* **2020**, *19*, 298. [[CrossRef](#)]
28. Cai, H.; Ren, Z. Resonance interaction between two two-level entangled atoms in cosmic string spacetime. *Class. Quantum Gravity* **2018**, *35*, 235014. [[CrossRef](#)]
29. De A Marques, G.; Furtado, C.; Bezerra, V.B.; Moraes, F. Landau levels in the presence of topological defects. *J. Phys. A Math. Gen.* **2001**, *34*, 5945. [[CrossRef](#)]
30. Poux, A.; Araújo, L.; Filgueiras, C.; Moraes, F. Landau levels, self-adjoint extensions and Hall conductivity on a cone. *Eur. Phys. J. Plus* **2014**, *129*, 100. [[CrossRef](#)]
31. Bueno, M.; Furtado, C.; Carvalho, A.D.M. Landau levels in graphene layers with topological defects. *Eur. Phys. J. B* **2012**, *85*, 53. [[CrossRef](#)]
32. Medeiros, E.F.; de Mello, E.B. Relativistic quantum dynamics of a charged particle in cosmic string spacetime in the presence of magnetic field and scalar potential. *Eur. Phys. J. C* **2012**, *72*, 2051. [[CrossRef](#)]
33. De Sousa Gerbert, P. Fermions in an Aharonov–Bohm field and cosmic strings. *Phys. Rev. D* **1989**, *40*, 1346–1349. [[CrossRef](#)]
34. Azevedo, S.; Pereira, J. Double Aharonov–Bohm effect in a medium with a disclination. *Phys. Lett. A* **2000**, *275*, 463–466. [[CrossRef](#)]
35. Reed, M.; Simon, B. *Methods of Modern Mathematical Physics. II. Fourier Analysis, Self-Adjointness*; Academic Press: New York, NY, USA; London, UK, 1975.
36. Gitman, D.; Tyutin, I.; Voronov, B. *Self-adjoint Extensions in Quantum Mechanics*; Birkhäuser Boston: Boston, MA, USA, 2012. [[CrossRef](#)]
37. Giri, P.R. Dipole binding in a cosmic string background due to quantum anomalies. *Phys. Rev. A* **2007**, *76*, 012114. [[CrossRef](#)]
38. Silva, E.O.; Andrade, F.M. Remarks on the Aharonov–Casher dynamics in a CPT-odd Lorentz-violating background. *Europhys. Lett.* **2013**, *101*, 51005. [[CrossRef](#)]
39. Andrade, F.M.; Silva, E.O. Effects of quantum deformation on the spin-1/2 Aharonov–Bohm problem. *Phys. Lett. B* **2013**, *719*, 467. [[CrossRef](#)]
40. Silva, E.O. On planar quantum dynamics of a magnetic dipole moment in the presence of electric and magnetic fields. *Eur. Phys. J. C* **2014**, *74*, 3112. [[CrossRef](#)]
41. Castro, L.B.; Silva, E.O. Quantum dynamics of a spin-1/2 charged particle in the presence of a magnetic field with scalar and vector couplings. *Eur. Phys. J. C* **2015**, *75*, 321. [[CrossRef](#)]
42. Park, D.K.; Oh, J.G. Self-adjoint extension approach to the spin-1/2 Aharonov–Bohm–Coulomb problem. *Phys. Rev. D* **1994**, *50*, 7715. [[CrossRef](#)]
43. Salem, V.; Costa, R.F.; Silva, E.O.; Andrade, F.M. Self-Adjoint Extension Approach for Singular Hamiltonians in $(2 + 1)$ Dimensions. *Front. Phys.* **2019**, *7*, 175. [[CrossRef](#)]
44. Gazeau, J.P. From classical to quantum models: the regularising rôle of integrals, symmetry and probabilities. *Found. Phys.* **2018**, *48*, 1648–1667. [[CrossRef](#)]
45. Bergeron, H.; Gazeau, J. Integral quantizations with two basic examples. *Ann. Phys.* **2014**, *344*, 43–68. [[CrossRef](#)]

46. Bergeron, H.; Gazeau, J.P. Variations à la Fourier-Weyl-Wigner on Quantizations of the plane and the Half-Plane. *Entropy* **2018**, *20*, 787. [[CrossRef](#)]
47. Gazeau, J.P.; Koide, T.; Noguera, D. Quantum smooth boundary forces from constrained geometries. *J. Phys. A Math. Theor.* **2019**, *52*, 445203. [[CrossRef](#)]
48. Bergeron, H.; Curado, E.M.F.; Gazeau, J.P.; Rodrigues, L.M.C.S. Quantizations from (P)OVM's. *J. Phys. Conf. Ser.* **2014**, *512*, 012032. [[CrossRef](#)]
49. Santos, L.; Barros, C. Scalar bosons under the influence of noninertial effects in the cosmic string spacetime. *Eur. Phys. J. C* **2017**, *77*, 186. [[CrossRef](#)]
50. Brandão, J.; Filgueiras, C.; Rojas, M.; Moraes, F. Inertial and topological effects on a 2D electron gas. *J. Phys. Commun.* **2017**, *1*, 035004. [[CrossRef](#)]
51. Muniz, C.; Bezerra, V.; Cunha, M. Landau quantization in the spinning cosmic string spacetime. *Ann. Phys.* **2014**, *350*, 105–111. [[CrossRef](#)]
52. Bakke, K. Rotating effects on the Dirac oscillator in the cosmic string spacetime. *Gen. Relat. Gravit.* **2013**, *45*, 1847–1859. [[CrossRef](#)]
53. Deng, L.F.; Long, C.Y.; Long, Z.W.; Xu, T. Generalized Dirac oscillator in cosmic string space-time. *Adv. High Energy Phys.* **2018**, *2018*. [[CrossRef](#)]
54. Zare, S.; Hassanabadi, H.; de Montigny, M. Non-inertial effects on a generalized DKP oscillator in a cosmic string space-time. *Gen. Relat. Gravit.* **2020**, *52*, 1–20. [[CrossRef](#)]
55. Hosseinpour, M.; Hassanabadi, H.; de Montigny, M. The Dirac oscillator in a spinning cosmic string spacetime. *Eur. Phys. J. C* **2019**, *79*, 311. [[CrossRef](#)]
56. Bakke, K.; Ribeiro, L.R.; Furtado, C.; Nascimento, J.R. Landau quantization for a neutral particle in the presence of topological defects. *Phys. Rev. D* **2009**, *79*, 024008. [[CrossRef](#)]
57. Lima, D.F.; Andrade, F.M.; Castro, L.B.; Filgueiras, C.; Silva, E.O. On the 2D Dirac oscillator in the presence of vector and scalar potentials in the cosmic string spacetime in the context of spin and pseudospin symmetries. *Eur. Phys. J. C* **2019**, *79*, 596. [[CrossRef](#)]
58. Andrade, F.M.; Silva, E.O. Effects of spin on the dynamics of the 2D Dirac oscillator in the magnetic cosmic string background. *Eur. Phys. J. C* **2014**, *74*, 3187. [[CrossRef](#)]
59. Hagen, C.R. Aharonov–Bohm scattering of particles with spin. *Phys. Rev. Lett.* **1990**, *64*, 503. [[CrossRef](#)] [[PubMed](#)]
60. Andrade, F.M.; Silva, E.O.; Pereira, M. Physical regularization for the spin-1/2 Aharonov-Bohm problem in conical space. *Phys. Rev. D* **2012**, *85*, 041701. [[CrossRef](#)]
61. Andrade, F.M.; Silva, E.O.; Pereira, M. On the spin-1/2 Aharonov-Bohm problem in conical space: Bound states, scattering and helicity nonconservation. *Ann. Phys.* **2013**, *339*, 510–530. [[CrossRef](#)]
62. Hagen, C.R. Exact equivalence of spin-1/2 Aharonov-Bohm and Aharonov–Casher effects. *Phys. Rev. Lett.* **1990**, *64*, 2347–2349. [[CrossRef](#)]
63. Bordag, M.; Voropaev, S. Charged particle with magnetic moment in the Aharonov–Bohm potential. *J. Phys. A* **1993**, *26*, 7637. [[CrossRef](#)]
64. Dabrowski, L.; Stovicek, P. Aharonov–Bohm effect with delta-type interaction. *J. Math. Phys.* **1998**, *39*, 47–62. [[CrossRef](#)]
65. Silva, E.O.; Andrade, F.M.; Filgueiras, C.; Belich, H. On Aharonov–Casher bound states. *Eur. Phys. J. C* **2013**, *73*, 2402. [[CrossRef](#)]
66. Silva, E.O.; Ulhoa, S.C.; Andrade, F.M.; Filgueiras, C.; Amorin, R.G.G. Quantum motion of a point particle in the presence of the Aharonov–Bohm potential in curved space. *Ann. Phys.* **2015**, *362*, 739. [[CrossRef](#)]
67. Gesztesy, F.; Albeverio, S.; Hoegh-Krohn, R.; Holden, H. Point interactions in two dimensions: Basic properties, approximations and applications to solid state physics. *J. Reine Angew. Math.* **1987**, *380*, 87. [[CrossRef](#)]
68. Adami, R.; Teta, A. On the Aharonov–Bohm Hamiltonian. *Lett. Math. Phys.* **1998**, *43*, 43–54. [[CrossRef](#)]
69. Bulla, W.; Gesztesy, F. Deficiency indices and singular boundary conditions in quantum mechanics. *J. Math. Phys.* **1985**, *26*, 2520. [[CrossRef](#)]
70. Albeverio, S.; Gesztesy, F.; Hoegh-Krohn, R.; Holden, H. *Solvable Models in Quantum Mechanics*, 2nd ed.; AMS Chelsea Publishing: Providence, RI, USA, 2004.
71. Aharonov, Y.; Bohm, D. Significance of Electromagnetic Potentials in the Quantum Theory. *Phys. Rev.* **1959**, *115*, 485. [[CrossRef](#)]

72. Hagen, C.R. Comment on “Relativistic Aharonov–Bohm effect in the presence of planar Coulomb potentials”. *Phys. Rev. A* **2008**, *77*, 036101. [[CrossRef](#)]
73. Abramowitz, M.; Stegun, I.A. (Eds.) *Handbook of Mathematical Functions*; Dover Publications: New York, NY, USA, 1972.
74. Andrade, F.M.; Silva, E.O.; Prudêncio, T.; Filgueiras, C. On Aharonov–Casher scattering in a CPT-odd Lorentz-violating background. *J. Phys. G* **2013**, *40*, 075007. [[CrossRef](#)]
75. Khalilov, V.R. Zero-mass fermions in Coulomb and Aharonov–Bohm potentials in 2 + 1 dimensions. *Theor. Math. Phys.* **2013**, *175*, 637–654. [[CrossRef](#)]
76. Khalilov, V. Creation of planar charged fermions in Coulomb and Aharonov–Bohm potentials. *Eur. Phys. J. C* **2013**, *73*, 2548. [[CrossRef](#)]
77. Khalilov, V.; Ho, C.L. Scattering of spin-polarized electron in an Aharonov–Bohm potential. *Ann. Phys.* **2008**, *323*, 1280–1293. [[CrossRef](#)]
78. Khalilov, V.R.; Mamsurov, I. Scattering of a neutral fermion with anomalous magnetic moment by a charged straight thin thread. *Theor. Math. Phys.* **2009**, *161*, 1503. [[CrossRef](#)]
79. Khalilov, V. Bound states of massive fermions in Aharonov–Bohm-like fields. *Eur. Phys. J. C* **2014**, *74*, 2708. [[CrossRef](#)]
80. Filgueiras, C.; Silva, E.O.; Oliveira, W.; Moraes, F. The effect of singular potentials on the harmonic oscillator. *Ann. Phys.* **2010**, *325*, 2529. [[CrossRef](#)]
81. Itzykson, C.; Zuber, J. *Quantum Field Theory*; Dover Books on Physics; Dover Publications: Mineola, NY, USA, 2012.

Publisher’s Note: MDPI stays neutral with regard to jurisdictional claims in published maps and institutional affiliations.



© 2020 by the authors. Licensee MDPI, Basel, Switzerland. This article is an open access article distributed under the terms and conditions of the Creative Commons Attribution (CC BY) license (<http://creativecommons.org/licenses/by/4.0/>).